University of Baghdad
College of Engineering
JOURNAL OF ENGINEERING

Journal of Engineering

journal homepage: www.joe.uobaghdad.edu.iq

Volume 29 Number 8 August 2023

Flexural Behavior of Reinforced Rubberized Reactive Powder Concrete Beams under Repeated Loads

Hussein Haider Mohammed[1,*], Ahmed Sultan Ali[2]

Department of Civil Engineering, College of Engineering, Al Nahrain University, Baghdad, Iraq
hussen_abed96@yahoo.com[1], Ahmed.s.ali@nahrainuniv.edu.iq[2]

ABSTRACT

Non-biodegradability of rubber tires contributes to pollution and fire hazards in the natural environment. In this study, the flexural behavior of the Rubberized Reactive Powder Concrete (RRPC) beams that contained various proportions and sizes of scrap tire rubber was investigated and compared to the flexural behavior of the regular RPC. Fresh properties, hardened properties, load-deflection relation, first crack load, ultimate load, and crack width are studied and analyzed. Mixes were made using micro steel fiber of the straight type, and they had an aspect ratio of 65. Thirteen beams were tested under two loading points (Repeated loading) with small-scale beams (1100 mm, 150 mm, 100 mm) size.

The fine aggregate is replaced by 5, 10, and 15%, respectively, with crumb rubber. While replacement of silica fume was 10, 20, 30, and 50%, respectively, with very fine rubber. Also, chip rubber was added to the mixture as coarse aggregate with 5, 10, and 15%. Five tested beams were chosen as case studies to analyze and compare the results of the ABAQUS software with the experimental results. The results showed that the flexural behavior of RRPC beams that contains rubber was acceptable when compared with the flexural behavior of the RPC beam (depending on load-carrying capacity). The crack width was decreased by including waste rubber and steel fibers. There is a satisfactory agreement between the results of the numerical analysis and the results of the experimental testing. Slight ultimate load differences are targeted between the effects of the monotonic loading and the repeated loading.

Keywords: Rubberized Concrete, Waste Tire Rubber, Flexural Tests, Finite Element Program, ABAQUS

**Corresponding author
Peer review under the responsibility of University of Baghdad.
https://doi.org/10.31026/j.eng.2023.08.03

Article received: 07/09/2022
Article accepted: 05/10/2022
Article published: 01/08/2023

سلوك الانثناء لعتبات خرسانة المساحيق الفعالة الممططة تحت تأثير الاحمال المتكررة

حسين حيدر محمد[1]،*، احمد سلطان علي[2]

قسم الهندسة المدنية، كلية الهندسة، جامعة النهرين، بغداد، العراق

الخلاصة

الاطارات المطاطية غير قابلة للتحلل في الطبيعة، تؤدي الى مشاكل بيئية مثل مخاطر الحرق. في هذا البحث، تمت دراسة سلوك الانثناء لعتبات الخرسانة ذات المسحوق التفاعلي التي تحتوي على نسب مختلفة واحجام مختلفة من المطاط الناتج عن نفايات الاطارات ومقارنتها بسلوك الانثناء للعتبة الخرسانية ذات المسحوق التفاعلي. تم فحص الخواص الجديدة والخواص المتصلبة وعلاقة الحمل بالتشوه وحمل الشق الأول والحمل النهائي وعرض الشق. تم استخدام الالياف الفولاذية الدقيقة (النوع المستقيم) مع نسبه الطول الى العرض 65. تم اختبار ثلاثة عشر عتبة تحت تحميل نقطتين (التحميل المتكرر) ذات مقياس مصغر (الطول 1100 ملم، الارتفاع 150 ملم، العرض 100 ملم). تم استبدال جزء من الركام الناعم بدلا من فتات المطاط بنسب 5 و10 و15%. وكما تم استبدال دخان السليكا بدلا من المطاط الناعم جدا بنسب 10 و20 و30 و50%. علاوة على ذلك، تمت اضافة رقائق المطاط الى الخليط كركام خشن بنسب 5 و10 و15%. تم اختيار خمسة من العتبات التي تم اختبارها بالمختبر لتحليلها باستخدام برنامج العناصر المحددة لمقارنة النتائج المختبرية مع التحليل العددي. اظهرت النتائج ان سلوك الانثناء للعتبات ذات المسحوق التفاعلي والمحتوية على نفايات المطاط كان مقبولا عند مقارنتها بسلوك الانثناء للعتبة ذات المسحوق التفاعلي (يعتمد على قدرة تحمل الحمولة). قل عرض الشقوق بإضافة نفايات الإطارات المطاطية والالياف الفولاذية. يظهر توافق مرضي بين نتائج التحليل العددي ونتائج الاختبارات المختبرية. اختلافات طفيفة في الحمل النهائي بين نتائج التحميل الرتيب والتحميل المتكرر.

الكلمات الرئيسية: الخرسانة المطاطية، نفايات الإطارات المطاطية، اختبار الانحناء، برنامج العناصر المحدودة، أباكوس.

1. INTRODUCTION

The stored used tires are slowly degrading under the effects of solar radiation. Degraded material would slowly contaminate soil and underground water over the years. Tires burn with thick black smoke and heat, quickly spread over the whole disposal area, and leave an oily residue that contaminates the soil. Many studies have been used in different types of scrap tires rubber by incorporating them with fine and coarse aggregates in concrete. Recycling waste as part of other processes can bring several benefits, including reducing energy usage, resolving landfill issues, and saving the consumption of natural resources (fine and coarse aggregate). It can also reduce the risks to human health and other creatures **(De Brito and Saikia, 2012)**. Reactive powder concrete can deliver ultra-high strength and low porosity cementitious material with improved mechanical and physical characteristics. That has high cement and silica fume contents, low water-binder ratios, and uses a new

generation of superplasticizers. RPC may also incorporate many steel or synthetic fibers, enhancing ductility and high durability. Unlike conventional concrete, RPC contains no coarse aggregate, and the fine aggregate is replaced by fine sand and crushed quartz **(Richard and Cheyrezy, 1994)**. In this context, **(Kadhum, 2015)** investigated an RPC cast using economical materials. Its mechanical properties were investigated and evaluated by studying the effects of using different cement and silica fume contents and local steel fibers as reinforcement for this concrete. The results showed that producing RPC from local materials is feasible by applying RPC principles and packing density theories. The use of fine sand whose grain size is (<600μm) improves the compressive strength due to the denser microstructure of the cement matrix. RPC without fibers is a brittle material and fails suddenly and violently. Adding fiber to concrete increases the resistance impact of the composite and changes its brittle failure mode into a more ductile one. Later, **(Wang et al., 2015)** employed two methods to alter the base mix Reactive Powder Concrete (RPC). They used a 40% equivalent volume substitution instead of fine sand in Mix B. Mix A maintains the base RPC mix and adds rubber up to 20.4 kg/m^3. Some specimens were subjected to heat cured. Two sizes of rubber crumbs were used, 0.6 and 2 mm, for each mix, A and B. The results showed that the hardened concrete density dropped when rubber particles replaced the same fine sand volume in the mixture. Both combined designs have a lower compressive strength. The Flexural behavior of the prism specimens can continue loading at much higher stress after the first cracking. However, when compared to the basic mixture, mix A only slightly decreases flexural strength, but mix B with a 40% substitution of fine sand shows a considerable drop. 60% of the strength of both the first and ultimate cracks was lost. **(Azhroul, 2017)** used crumb rubber and micro-waste rubber powder (micro WRP) as fine aggregate to replace the-conventional sand in UHPC. The replacement levels of crumb rubber and micro WRP comprise 0, 10, 20, 30, 40, and 50% based on the weight of the fine aggregate utilized. The outcomes showed that the addition of crumb rubber and micro WRP into the UHPC mix led to the reduction of workability and compressive strength. And increasing the percentage of crumb rubber and micro WRP as a partial replacement for sand decreased the followability of the concrete**. (Kammash and Abdul-Husain, 2022)** investigated eighteen specimens, the bond strength between a reinforcing bar and rubberized concrete was produced by adding waste tire rubber instead of natural aggregate. The fine and coarse aggregate was replaced in 0%, 25%, and 50%, respectively, with the small pieces of a waste tire. The experimental results reported that a reduction of 19% in bond strength was noticed in 50% of replaced rubberized concrete compared with conventional concrete. The bond strength of the rubberized concrete increased when the concrete cover, compressive strength of the concrete, and the yield stress of rebar were increased. The failure modes in rubberized concrete are similar to that of conventional concrete. **(Ishak, 2018)** replaced the amount of aggregate with waste crumb tire (WCT) in the UHPC mix. The weight of the WCT was reduced by 5%. The WCT was pre-treated by soaking the WCT granules in NaOH solution for 20, 40, and 60 minutes, respectively. A 3% NaCl solution was used to wash the UHPC specimens. According to the results, the

compressive strength of rubberized UHPC (RUHPC) was much lower than that of plain UHPC. Compared to conventional UHPC, the chloride penetration depth of RUHPC was greater. The chloride penetration depth of UHPC-20 is larger than that of UHPC-40 and UHPC-60 in the RUHPC. The UHPC-60 improved chloride-resistant penetration more than others. **(Pham et al., 2021)** incorporated Rubberized Reactive Powder Concrete RRPC of 2% by volume of steel fibers. Rubber has a maximum particle size of 0.6 mm. Silica sand (0.3 mm) was replaced by rubber powder by 0, 10, 20, and 40% by the volume in the mix. When the rubber component was increased from 0 to 40%, the results revealed that the RRPC compressive strength decreased from 136.1 MPa to 67.8 MPa. This was because of the poor ITZ of both rubber and cement. The percentage of strength reduction in the RRPC was lower than that of the high and normal Rubberized Concrete for the same rubber content. This demonstrates that the marriage of RPC and rubber powder might be agreeable to other types of RC. In the production of RPC content. **(Zhang et al., 2022)** substituted the same volume of river sand with three different proportions of rubber powders at 5, 10, and 15%, respectively. The results showed that the increase in rubber powders reduced the flow, compressive strength, and Flexural prism strength of RRPC. Due to insufficient adhesion between rubber powder and cement paste, the quasi-static mechanical characteristics of RRPC were severely impaired. The level of damage and the brittle behavior of RRPC under loading was greatly reduced when there was a higher concentration of rubber granules in the material.

The main aim of the present study is to produce successful mixes of Rubberized Reactive Powder Concrete (RRPC) in fresh and hardened properties (using waste tires rubber). Also possibility of investigating the effect of using various amounts of waste tire rubber as a replacement for the percentages of 5, 10, and 15% by volume of fine aggregates at 10, 20, 30, and 50% by weight of silica fume. Furthermore, to show the effect of Chip Rubber added to RPC mixes with percentages (5, 10, and 15%) as Coarse Aggregates (by weight) without steel fiber on the behavior of the supported beams under monotonic and repeated loading to obtain environmentally friendly and sustainable concrete. In addition, the behavior of supported beams under flexural loading using the finite element program (ABAQUS) is also investigated.

2. EXPERIMENTAL STUDY

2.1 Materials Properties

All the mixes were made with Portland cement (V) sulfate-resistant. The sand (zone 2) was used depending on **(IQS No. 45/1984)**. The specific gravity of the aggregate was 2.60. No coarse aggregate. Silica fume, which looks like a grey powder, was used as a pozzolanic filler. Silica fume was tested physically and chemically and met the standards of **(ASTM C1240-15)**. A Superplasticizer (SP) with a PH value of 6 and specific gravity of 1.1 was utilized to reduce water, flow ability, viscosity, and high early strength. As shown in **Fig. 1**, microfiber has a length of 13 mm, an aspect ratio of 65, a volume fraction (Vf = 2%), and a tensile strength of 2600 Mpa. Different sizes and shapes of scrap tire rubber were employed; chip

rubber with a size range of 1.18-9.5 mm was used and added to the mixture as coarse aggregate, crumb rubber with a size range of 0.15-4.75 mm was also used to replace fine aggregate, and finally, a very fine rubber with a particle size of 2.5 microns was used to replace of silica fume. The various sizes of waste rubber with a specific gravity of 1.78 and water absorption of 2% were provided by the General Agency for Rubber Products and Tires/Iraq **Fig. 2**. Two different sizes of steel bar reinforcement (Ø6mm and Ø4mm) were utilized to reinforce the beams. The yield tensile stress of these beams was 548 MPa and 565 MPa, respectively, as specified in the **(ASTM A496-07)**.

Figure 1. Micro steel fiber.

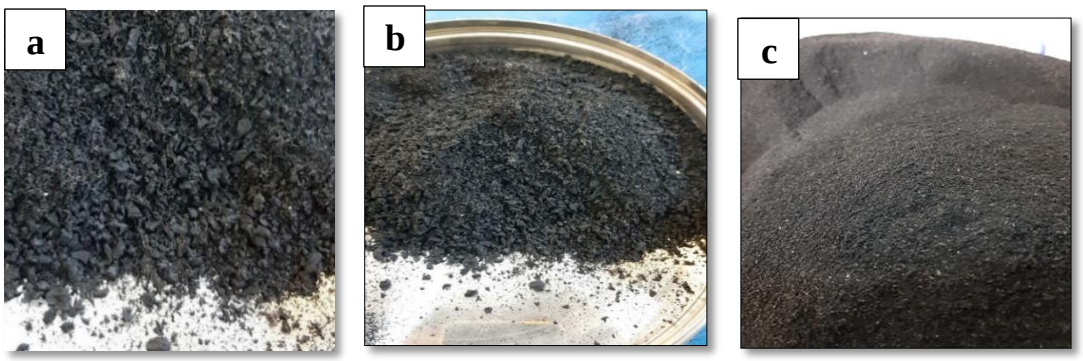

Figure 2. Types of tire rubber: (a) chip rubber, (b) crumb rubber, (c) very fine rubber.

2.2 Concrete Mixes

Several trial mixes were performed to acquire effective mixes in fresh characteristics for RRPC (workability), and the mixes were intended for structural concrete since achieving good mixes in mechanical properties for RRPC (rubberized reactive powder concrete) is highly challenging. The lab work involves the creation of thirteen different mixtures; (RPC, RRPC with 15%, 10%, and 5% of the fine aggregate instead of Crumb rubber, RRPC with 15%, 10%, and 5% of chip rubber added to the mixture as coarse aggregate, RRPC with 50%, 30%, 20% and 10% of silica fume was used instead of very fine rubber). **Table 1** shows information about the blends that were used.

Table 1. Details of mixes.

Beam No.	Mixes	Cement kg/m^3	Fine Aggregates kg/m^3	Chip Rubber kg/m^3	Crumb Rubber kg/m^3	Silica Fume kg/m^3	Very Fine Rubber kg/m^3	Micro Steel Fiber kg/m^3	Superplasticizer l/100 kg	Water Binder l/m^3
B1	RPC	1062	1328	-	-	266	-	156	5.5	214
B2	RPC	1062	1328	-	-	266	-	156	5.5	214
B3	FA5	1062	1261	-	67	266	-	156	5.7	236
B4	FA10	1062	1195	-	133	266	-	156	5.8	241
B5	FA15	1062	1128	-	200	266	-	-	5.9	245
B6	FA15S	1062	1128	-	200	266	-	156	6.1	256
B7	CA5	1062	1328	33	-	266	-	-	6.1	228
B8	CA10	1062	1328	65	-	266	-	-	6.3	231
B9	CA15	1062	1328	98	-	266	-	-	6.4	248
B10	SF10	1089	1328	-	-	239	27	156	5.6	216
B11	SF20	1116	1328	-	-	212	54	156	5.8	218
B12	SF30	1142	1328	-	-	186	80	156	5.8	221
B13	SF50	1195	1328	-	-	133	133	156	5.9	226

2.3. Tests of Fresh Concrete

Fresh properties of RPC and RRPC are studied by conducting a flow table test, as shown in **Fig.3**. Flow table test is most commonly used to assess the horizontal flow (flowing ability) of concrete mix, a suitable test to determine the workability for all types of concrete mixtures. It was done in compliance with the **(ASTM C1437-15)** standard.

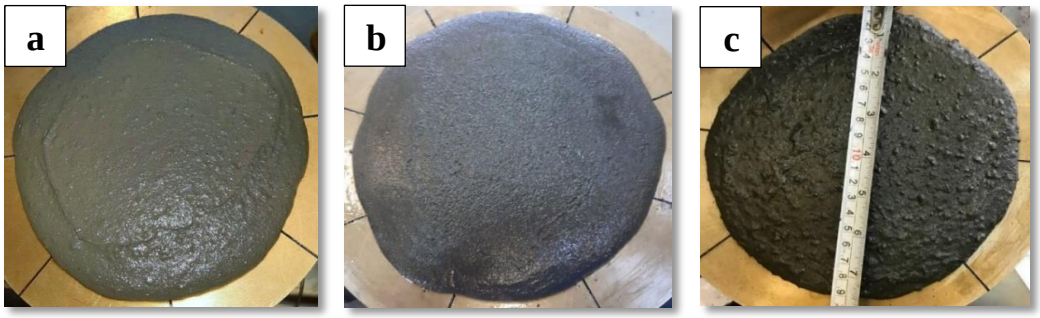

Figure 3. Flow table test: (a) FA10, (b) SF10, (C) CA10

The workability of the Rubberized Reactive Powder concrete mix (RRPC) lowered due to the inclusion of micro steel fibers in the composite. Microfiber makes the mixture harder to work with and makes the friction in both the aggregates and microfibers worse, obstructing the motion of the mixture. Using various percentages of rubber also negatively affects the ease of movement because the rubber particles' low specific gravity compared to the specific gravity of other materials reduces the mix mobility. The results also showed that the

diameter of the flow table of RRPC with crumb rubber was higher than that of chip rubber. The micro steel fibers and rubber particles raised the water-cement ratio (w/b) and Superplasticizer dose. These results are listed in **Table 2**.

2.4. Tests of Hardened Concrete

A (100x100x100) mm cube and a (100x200) mm cylinder were utilized to test the compressive and tensile strength at 28 days, as specific to **(BS 1881: part 116: 1997)** and **(ASTM C496-17)**, respectively. Depending on **(ASTM C348-21)**, the modulus of the rupture test was also done with a (100x100x600) mm prism.

The findings demonstrate that the compressive strength decreases as the rubber content increases. The decrease was about 12.8, 18.7, 52.2, 41.1, 11.3, 20.0, and 35.9% for mixes FA5, FA10, FA15, FA15S, CA5, CA10, and CA15, respectively, compared with reference mix (RPC).

Table 2. Fresh tests result from different mixes.

No.	Mix Code	Superplasticizer Dosage (l/100 kg)	Flow Table (mm)	W/B Ratio
1	RPC Ref.	5.5	100	0.16
2	FA5	5.7	101	0.18
3	FA10	5.8	99	0.18
4	FA15	5.9	98	0.18
5	FA15S	6.1	97	0.19
6	CA5	6.1	98	0.17
7	CA10	6.3	96	0.17
8	CA15	6.4	95	0.19
9	SF10	5.6	101	0.16
10	SF20	5.8	100	0.16
11	SF30	5.8	98	0.17
12	SF50	5.9	97	0.17

The softness of leftover tire rubber granules compared to aggregates or other materials is the cause for this decrease. Waste rubber and paste of cement have poor adherence (the area where the rubber particles and cement paste meet has poor strength). The results also noticed that the compressive strength in rubber replaced with the silica fume had decreased significantly. Compared with the reference mix (RPC), the reduction in compressive strength was about 10.5, 21.6, 38.2, and 50.0% for mixes SF10, SF20, SF30, and SF50, respectively. This has happened because the surface area of rubber particles is less than that of the silica fume, resulting in an abundance of cement paste.

Moreover, the size of rubber particles (2.5 μm) is greater than that of silica fume particles. Therefore, all sizes void in the mix were blocked. The same ended reasons that made the splitting tensile and flexural strength weaker also made the compressive strength weaker. **Table 3** shows the results of the hardened concrete tests.

2.5. Flexural Test Setup and Instrumentation

Deformed bars are used to strengthen thirteen beams. Two bars were used for main reinforcement (Ø6mm) and two for compression reinforcement (Ø4mm). (4 and 56mm c/c) was utilized to stop failure in shear. Each beam was 1100 mm long, 150mm high, and 100mm wide. Beams were made to break at bending as specified **(Committee, 2019)**. Two kinds of loads were put in to test the beams (monotonic and repeated loading). In **Table 4**, the name and definition of the beam are shown. **Fig. 4** shows the dimension of the beams as well as the specification of the reinforcement.

Table 3. Results of the hardened concrete tests.

Mixes	Compressive strength (MPa)	Splitting strength (MPa)	Modulus of rupture (MPa)
RPC	101.0	11.84	17.50
FA5	88.07	10.56	14.73
FA10	82.11	9.03	13.44
FA15	48.27	5.02	12.11
FA15S	59.48	6.54	12.68
CA5	89.58	8.98	13.82
CA10	80.81	8.24	12.54
CA15	64.73	6.67	11.87
SF10	90.39	10.84	16.26
SF20	79.18	8.82	15.40
SF30	62.41	7.42	13.95
SF50	50.51	5.80	11.37

Table 4. Beams designation and description.

No.	Mix Designation	Description
1	RPC	Reactive Powder Concrete with fiber
2	RPC	Reactive Powder Concrete with fiber
3	FA5	RPC + 5% of Fine Sand replace by crumb rubber with fiber
4	FA10	RPC + 10% of Fine Sand replace by crumb rubber with fiber
5	FA15	RPC + 15% of Fine Sand replace by crumb rubber without fiber
6	FA15S	RPC + 15% of Fine Sand replace by crumb rubber with Fiber
7	CA5	RPC + 5% Chip rubber Added without fiber
8	CA10	RPC + 10% Chip rubber Added without fiber
9	CA15	RPC + 15% Chip rubber Added without fiber
10	SF10	RPC + 10% of Silica Fume replace by very fine rubber with fiber
11	SF20	RPC + 20% of Silica Fume replace by very fine rubber with fiber
12	SF30	RPC + 30% of Silica Fume replace by very fine rubber with fiber
13	SF50	RPC + 50% of Silica Fume replace by very fine rubber with fiber

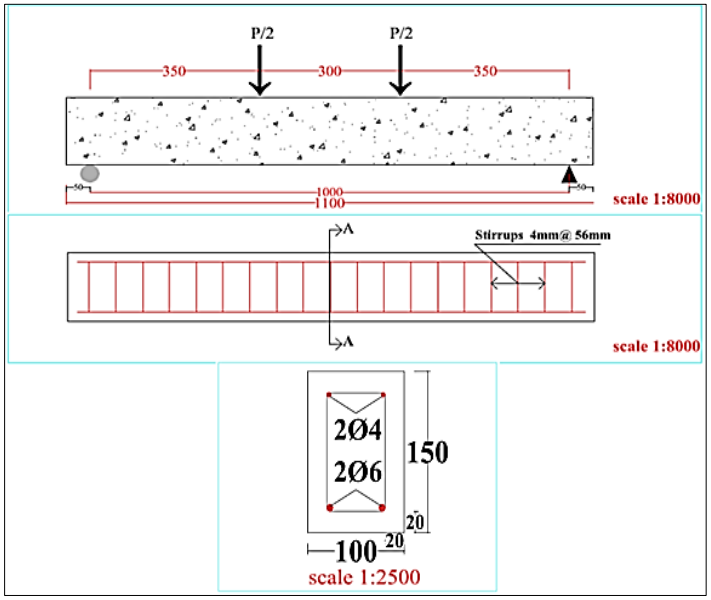

Figure 4. Beam dimensions and reinforcement details.

2.5.1 Flexural Test Results of the Beams

Table 5 shows the results of testing the beams from bending strength. **Figs. 5** and **6** show the examination results as bar charts.

Table 5. Results of the flexural test (Flexural Failure type).

Beam No.	Beam designation	Group	Test	Load at first crack (kN)	Deflection at the first crack (mm)	Load at Failure (kN)	Deflection at Failure (mm)	Number of crack At failure	Crack width (mm)
B1	RPC	G1	Monotonic	15.41	0.48	33.35	4.77	8	0.08-0.20
B2	RPC		Repeated	14.00	0.40	31.11	4.41	9	0.06-0.20
B3	FA5		Repeated	12.44	0.58	27.25	4.45	8	0.05-0.18
B4	FA10		Repeated	11.52	0.70	26.00	5.88	7	0.04-0.10
B5	FA15		Repeated	6.41	0.58	18.31	5.40	8	0.08-0.12
B6	FA15S		Repeated	10.50	0.74	25.72	6.52	8	0.04-0.18
B7	CA5	G2	Repeated	8.00	0.58	16.89	6.51	9	0.06-0.12
B8	CA10		Repeated	7.56	0.70	14.56	6.24	7	0.08-0.16
B9	CA15		Repeated	7.00	0.84	13.84	5.51	9	0.08-0.18
B10	SF10	G3	Repeated	11.51	0.70	25.42	5.47	9	0.03-0.16
B11	SF20		Repeated	10.42	0.78	24.35	5.21	8	0.02-0.08
B12	SF30		Repeated	10.00	0.81	22.51	4.95	8	0.01-0.05
B13	SF50		Repeated	9.14	0.90	20.14	4.11	8	0.01-0.04

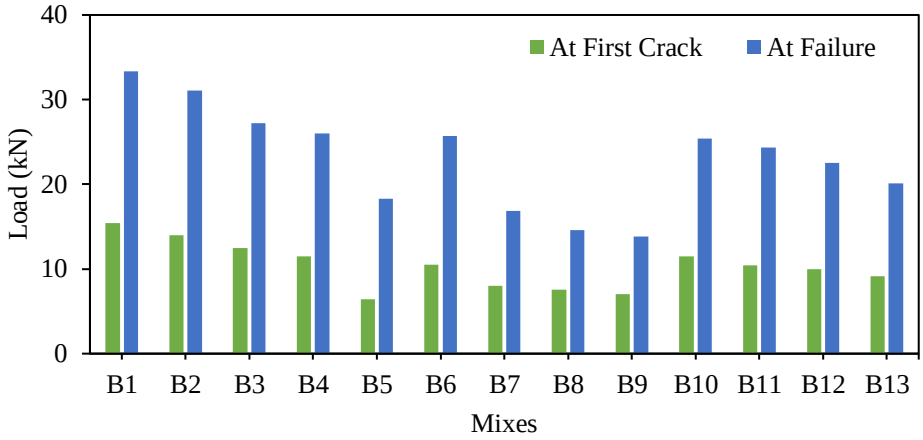

Figure 5. Load at first crack and failure.

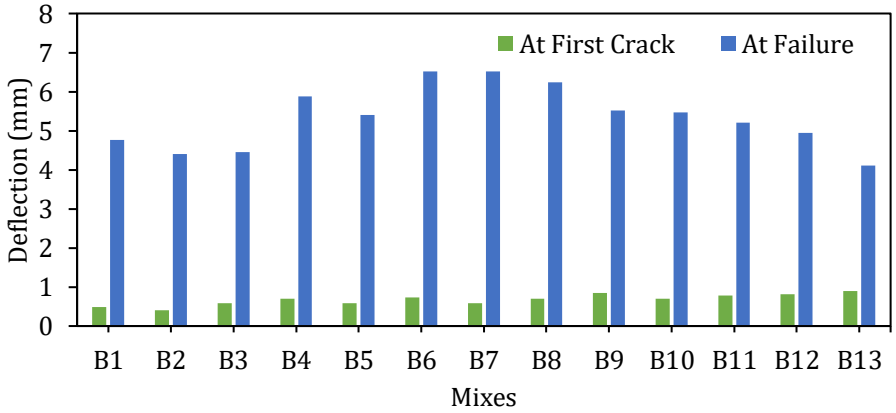

Figure 6. Deflection at first crack and failure.

As shown in **Fig. 7**, all of the beams have the same pattern of cracks; flexural failure was the pattern detected. All beams developed minor perpendicular cracks at the center in the initial testing phase. Load increased the amount of cracks. The findings showed that adding microfiber and rubber granules decreased the fracture's breadth because the micro steel fiber prevented the cracks and limited their expansion **(Asaad et al., 2017)**. In addition, the granules of rubber can absorb more energy.

2.5.2 Modes of Failure for the Tested Beams

The history of the loading (cyclic non-reversed load) shown in **Fig. 8** was used on the samples. The load history was proposed by **(FEMA, 2007)**. The loading-unloading process caused a fluctuation of stresses, and much damage appeared in the structures (flexural cracks in beams, higher deflection, etc.) compared to the monotonic loading. A typical failure pattern in the flexural failure of the repeated beam samples was similar to that in the monotonic beam samples.

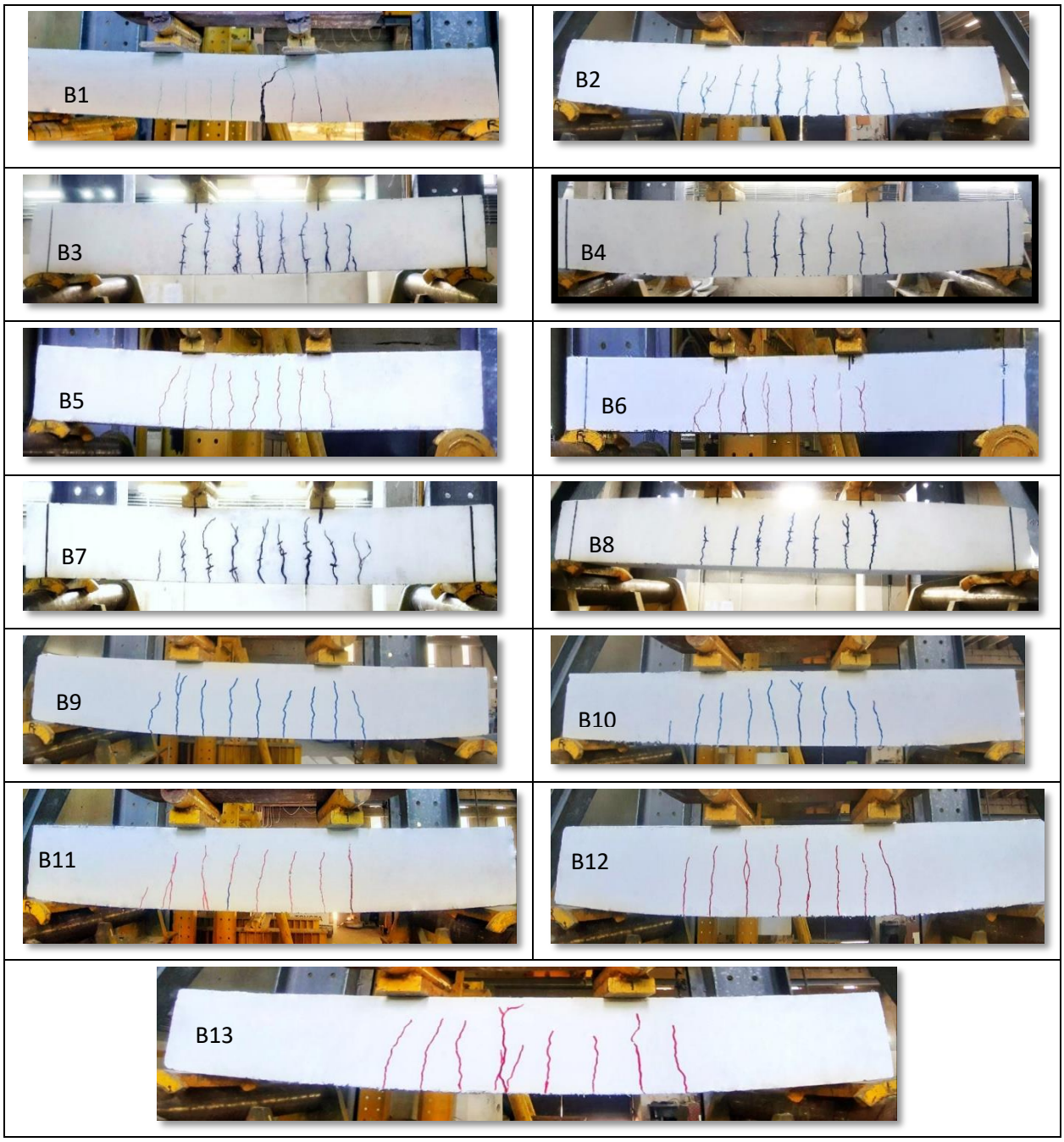

Figure 7. Beams after testing.

The results showed that the failure load capacity decreased as compared to the reference RPC beam (B2); the reductions were about 12.4, 16.4, 41.1, and 17.3% for B3, B4, B5, and B6, respectively. The decrease in failure load was related to the presence of rubber particles. The presence of micro steel fibers limited this reduction. A higher reduction was recorded for B5 since it did not have micro steel fibers. In addition, the results showed that the rubber particles improved the deformation, so the deflection at failure increased by about 0.9, 33.3, 22.4, and 47.8% for B3, B4, B5, and B6, respectively. From these results, it can be concluded that the ultimate load decreased as rubber content increased. Deflection at failure increased as rubber content increased.

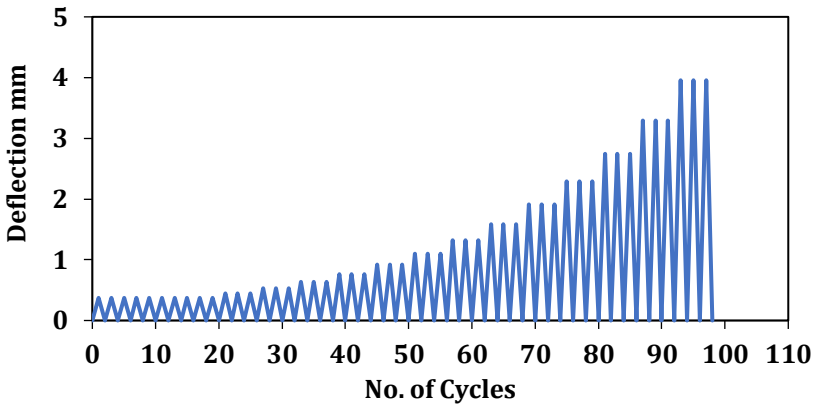

Figure 8. Load history used in FEA.

Beams B7, B8, and B9 have chip rubber without steel fiber. The results showed that the failure load capacity decreased compared to the reference RPC beam (B2); the reductions were about 45.7, 53.2, and 56.6% for B7, B8, and B9, respectively. This is because the chip rubber particles are weak and compressed, and the loading capacity will be reduced due to its impact on the strength of other concrete components. The blanks are also increased by chip rubber mixtures which negatively affect the failure load capacity. The absence of micro steel fibers was limiting this decrease. The results also showed that the rubber particles improved the deformation, so the deflection at failure increased by 47.6, 41.4, and 24.9% for B7, B8, and B9, respectively.

In the tested beams containing very fine rubber with micro steel fibers under repeated loading, the results showed that the failure load capacity decreased compared to the reference RPC beam (B2). The reductions were about 18.2%, 21.7%, 27.6%, and 35.2% for B10, B11, B12, and B13, respectively. This was attributed to the loss in silica fume reaction when replaced by rubber particles. The forming of the gel (C-S-H) had become less due to the low percentage of silica fume. Pozzolanic materials improved the paste bond and led to an increase in strength. The results also showed that the rubber particles improved the deformation, so the deflection at failure increased by 24.0, 18.1, and 12.2% for B10, B11, and B12, respectively. This improvement was due to the presence of rubber particles and little loss in pozzolanic reaction for silica fume. It is also due to the presence of steel fiber that increased the cohesion of the concrete components and reduced the occurrence of cracks. The reaction of pozzolanic can be shown as follows:

Pozzolanic + Calcium Hydroxide Ca(OH) + Water (H_2O) → Gel (C-S-H)

3. FINITE ELEMENT ANALYSIS

3.1 Element Type

The relevant sections describe the element types utilized to model S.S beams with ABAQUS **(CAE Abaqus, User's Manual, 2011)**:

3.1.1 Modeling of the Materials

Three-dimensional finite elements are employed to model beams. The basic 3D stress elements can be used to design concrete in ABAQUS. Concrete beams are made with a C3D8R element, a linear brick with 8 nodes. The C3D8R element's assimilation point is in the center of the element.

The 8-node brick element with the integration point is shown in **Fig. 9**. To design the steel bar reinforcement, a linear 3D two-node truss element (T3D2) with three freedom degrees at each node is utilized.

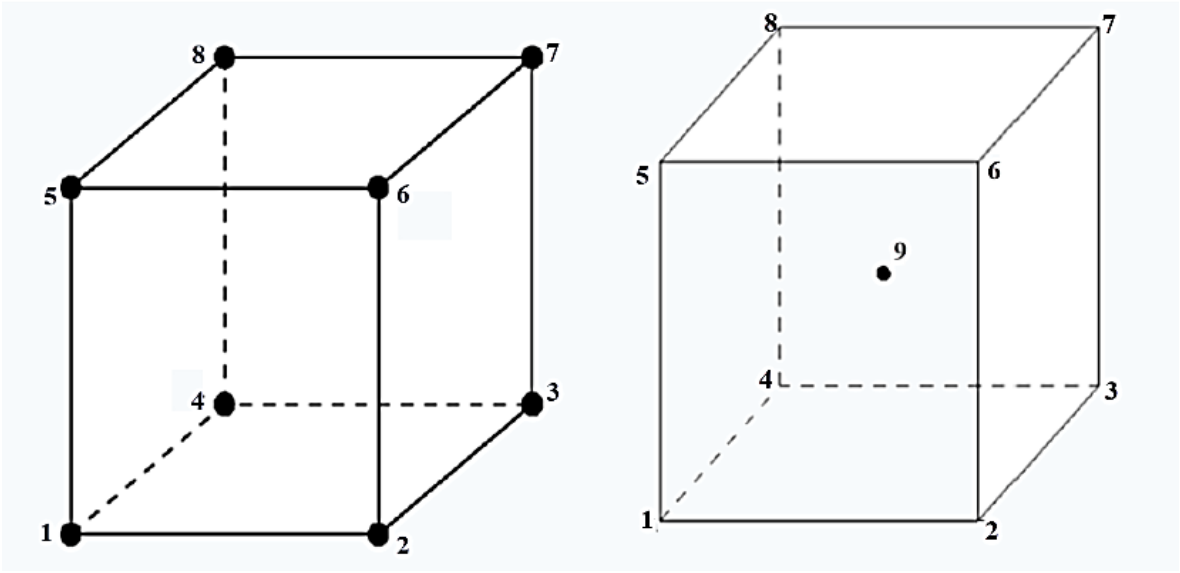

Figure 9. Eight-noded brick element with the integration point.

3.1.2 Modeling of Rubber and Steel Fiber

In material modeling, the concrete damage plasticity (CDP) model is used to model concrete, and the steel is modeled as elastic perfectly plastic. The steel fiber and rubber concrete were modeled within the modeling of the concrete properties CDP. For modeling Reactive Powder Concrete with steel fiber use, a stress-strain relation suggested by **(Collins et al., 1993)** was used. To provide efficient modeling for the structural behavior of concrete as follows:

$$\frac{f_c}{f_c'} = \frac{n(\varepsilon_{cf}/\varepsilon_c')}{n-1+(\varepsilon_{cf}/\varepsilon_c')^{nk}} \quad (1)$$

where f_c' is peak stress obtained from the cylinder test, ε_c' is strain when f_c reaches f_c', n is the curve fitting factor equal to $E_c/(E_c - E'_c)$, E_c is tangent stiffness when ε_{cf} is zero, E'_c is secant stiffness when ε_{cf} is ε_c', and k model the strain decay before and after experiencing peak stress. n and k are suggested by using data from high-strength concrete, and it was decided to use these two variables without change. n and k can be calculated by using

$$n = 0.8 + \frac{f_c'}{17} \quad (2)$$

$$k = 0.67 + \frac{f_c'}{62} \quad (3)$$

Using a constitutive model stress-strain relation by (Aslani et al., 2018) was used for modeling Rubber in Concrete. Input parameters are compressive strength. f_c obtained on reference concrete

cubic specimens, relative volumetric rubber ratio ρ_{vr}, and the size of the replaced aggregate $d_{g,repl}$ considered with factor λ. With known input parameters, it is possible to calculate the peak compressive stress for the rubberized concrete:

$$f_{rc} = \frac{1}{1+2\cdot\left(\frac{3\lambda\rho_{vr}}{2}\right)^{3/2}} f_c \quad (4)$$

The tangent elastic modulus for rubberized concrete:

$$E_{rc} = \frac{0.4 f_c}{\varepsilon_{el}} \cdot \exp(-\lambda\rho_{vr}) \quad (5)$$

The coefficient for calculating strain at peak stress:

$$v = \frac{f_{rc}}{17} + 0.8 \quad (6)$$

Strain at peak stress for rubberized concrete:

$$\varepsilon_{rc} = (f_{rc}/E_{rc})\left(\frac{v}{v-1}\right) \quad (7)$$

Secant modulus of elasticity:

$$E_p = f_{rc}/\varepsilon_{rc} \quad (8)$$

Coefficients of the linear equation:

$$\varphi = 35 \times (12.4 - 1.66 \times 10^{-2} f_{rc})^{-0.9} \quad (9)$$

$$\kappa = 0.75\exp\left(-\frac{911}{f_c}\right) \quad (10)$$

Modified material parameter:

$$\rho_m = \left[1.02 - 1.17\left(E_p/E_{rc}\right)\right]^{-0.74} + (\varphi + \kappa) \quad (11)$$

Stress factor to obtain the constitutive curve:

$$\frac{\sigma}{f_{rc}} = \left[\frac{\rho_m(\varepsilon/\varepsilon_{rc})}{\rho_m - 1 + (\varepsilon/\varepsilon_{rc})^{\rho_m}}\right] \quad (12)$$

The constitutive model of rubberized concrete was used, shown in **Fig. 10**.

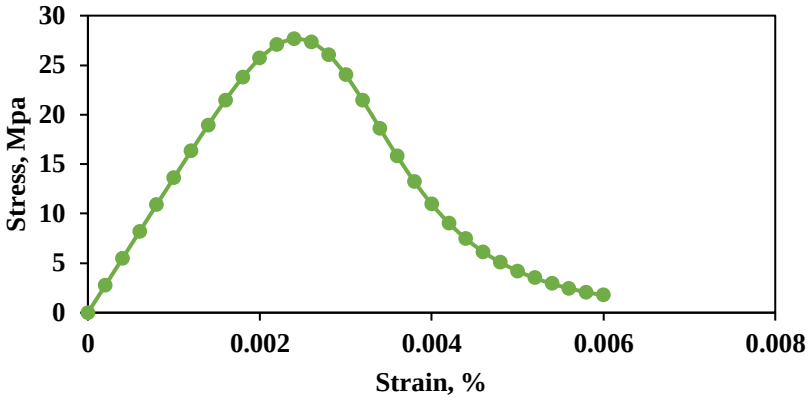

Figure 10. Constitutive model stress-strain curve

3.2 Input Data

This program used the parameters gathered from experiments as compressive strength and splitting tensile strength of the concrete. Modulus of elasticity and stress-strain curve were obtained from equations. All parameters are listed in **Tables 6** and **7** for all beams.

Table 6. Input data for steel reinforcement.

Parameter	Ø4 mm	Ø6 mm
Area of steel reinforcement (mm^2)	12.56	28.27
Yield strength (MPa)	565	548
Modulus of elasticity (MPa)	200000	200000
Poisson's ratio	0.2	0.2

ABAQUS default values were utilized for the additional required parameters, including eccentricity, $\boldsymbol{\sigma bo/\sigma co}$, dilation angle, kc, and the viscosity parameter. After a large number of trials, the amount of friction that exists between the concrete and the supports was determined. These tests aimed to find the number that minimized the gap in performance between the practical and the finite element results.

Table 7. Input data for beams.

Parameter	RPC Ref.	FA15S	CA5	SF10
Compressive strength (MPa) at the edge of the Beam	104.7	67.38	59.95	89.06
Splitting tensile strength (MPa) at the edge of the Beam	11.98	7.45	9.71	11.34
Modulus of elasticity (MPa)	40872	34153	32606	38232
Poisson's ratio for concrete	0.18	0.18	0.18	0.18
Dilation angle	50	40	40	45
Eccentricity	0.1	0.1	0.1	0.1
$\boldsymbol{\sigma bo/\sigma co}$	1.16	1.16	1.16	1.16
K	2/3	2/3	2/3	2/3
Viscosity parameter	0.001	0.001	0.001	0.001

3.3 Three-Dimensional Finite Element Meshes

The specimen was broken up into several tiny finite elements with the greatest size of 15 mm, as seen in **Fig. 11**. The design of steel bars appears in **Fig. 12**. The specimens were S.S supported at both sides, and one of the sides was formed into a roller by putting restraints on the Y-axis (with UY set to zero). By exerting restraints in the X, Y, and Z axes (UY=UX=UZ=zero), illustrated in **Fig.12**, another support was placed as a hinge.

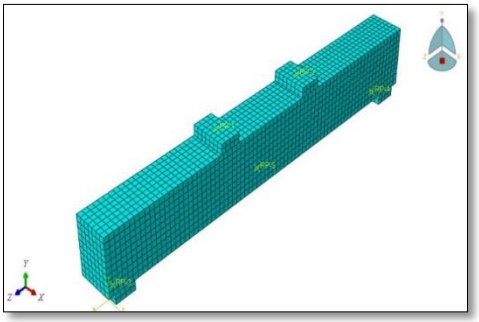

Figure 11. Mesh Configuration of FE Model

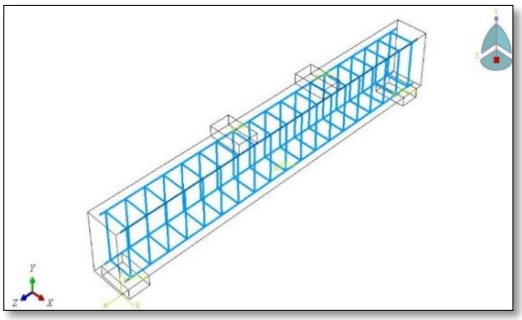

Figure 12. Boundary Conditions and reinforcement

3.4 Finite Element Analysis Results

The FEA results for the tested beams are shown in **Table 8**. In addition, the percentages of the laboratory and the numerical results are shown in this table. **Fig. 13** shows the load-deflection curves of the beams from the experimental test and finite element analysis. In general, the load-deflection curves of beams from the FEA results agree with the experimental results throughout the entire range of behavior.

Table 8. Experimental and FEA Results of Ultimate Loads and Corresponding Displacements

NO.	Beam Symbol	Load Type	Exp. Results		FEA Results		$\frac{Pu\ EXP}{Pu\ FEA}$	$\frac{\Delta u\ EXP}{\Delta u\ FEA}$
			Pu (KN)	Δu (mm)	Pu (KN)	Δu (mm)		
1	RPC Ref.	M	33.35	4.77	34.21	4.86	0.974	0.981
2	RPC Ref.	R	31.11	4.41	31.89	4.48	0.975	0.984
3	FA15S	R	25.72	6.52	23.25	6.63	1.106	0.983
4	CA5	R	16.89	6.51	17.79	6.23	0.949	1.044
5	SF10	R	25.42	5.47	21.95	5.58	1.158	0.980

The ratio of the ultimate experimental load to the FEA load ($P_{U\ EXP}/P_{U\ FEA}$), value is (1.032 on average) and the ratio of the experimental deflection to FEA deflection ($\Delta_{U\ EXP}/\Delta_{U\ FEA}$) is (0.984 on average). This ratio shows a good prediction of FEA results with experimental results for all modeled beams in the monotonic and repeated tests.

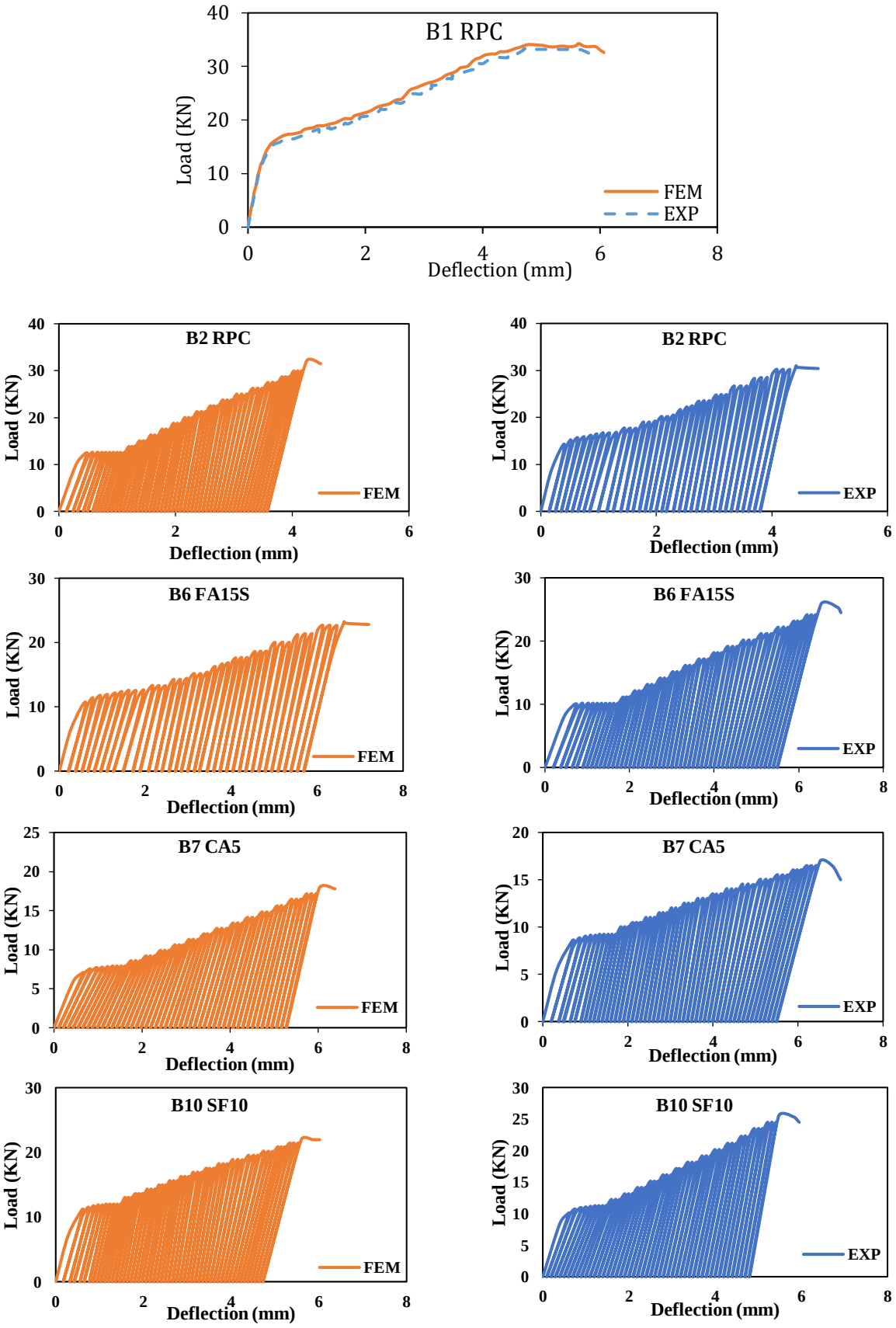

Figure 13. Numerical load-deflection curve for monotonic and repeated FEM loads

4. CONCLUSIONS

By following the methodology presented in this research, several conclusions have been obtained, as highlighted in the followings:

1. The Reactive Powder Concrete's fresh properties (Flow Table Test) generally decreased by combining microfibers and waste rubber granules. But the workability stayed under the acceptance criteria. The flow of the rubberized concrete test ranged from 100 ± 5 mm.
2. The Mechanical properties (compressive strength, splitting tensile strength, and modulus of rupture) reduced as rubber content increased when fine aggregates were substituted with crumbs and added chip waste rubber to the mixture.
3. The optimum percentage of the granules of the rubber substituted was 15% for fine aggregates, 10% for silica fume, and 5% for added chip rubber (depending on the results of fresh properties, hardened properties, and behavior of beams).
4. Substituting the granules of the rubber rather than the fine aggregate were superior compared to adding chip rubber as a coarse aggregate.
5. The addition of rubber granules and micro steel fibers changed the brittle behavior of failure of the tested beams to a ductile behavior failure.
6. The results obtained for modeled beams under monotonic and repeated loading using the finite element models are similar to those observed in the experimental work and have obtained a good agreement.
7. In the tested beams containing crumb rubber with micro steel fibers, the results showed that the rubber particles improved the deformation, and the presence of the micro steel fibers increases the cohesion of concrete components and reduces the occurrence of cracks.
8. The tested beams containing chip rubber without micro steel fibers showed that the failure load capacity decreased; the reductions were about 45.7%, 53.2%, and 56.6% for B7, B8, and B9, respectively. This is because the chip rubber particles are weak and compressed and the loading capacity will be reduced due to its impact on the strength of other concrete components.
9. In the tested beams that contain very fine rubber with micro steel fibers, the results showed that the failure load capacity decreased compared to the Ref. beam (B2); this was attributed to the loss in silica fume reaction when replaced by rubber particles (the forming of the gel (C-S-H) had become less due to the low percentage of silica fume).
10. Rubber particles improved the deformation, so the deflection at failure increased by 24.0%, 18.1%, and 12.2% for B10, B11, and B12, respectively. This improvement was due to the presence of rubber particles and little loss in the silica fume pozzolanic reaction.
11. For all beams, the results observed that the deformability and ductility indices increased with rubber content increased, and the ultimate load decreased as rubber content increased.

REFERENCES

Asaad, Z., Ghanim, G., Lecture, A., and Al-Quraishi, H., 2017. Compressive strength of bottle-shaped compression fields of fiber reinforced concrete members. *Journal of Engineering,* 23(11), pp. 56-69. Doi:10.31026/j.eng.2017.11.05

Aslani, F., Ma, G., Yim Wan, D.L., and Tran Le, V.X., 2018. Experimental investigation into rubber granules and their effects on the fresh and hardened properties of self-compacting concrete. *Journal of Cleaner Production*, 172, pp. 1835–1847. Doi:10.1016/j.jclepro.2017.12.003.

ASTM C1240, 2015. Standard specification for silica fume used for cementitious mixtures, ASTM International, West Conshohocken.

ASTM A496, 2007. Standard specification for steel wires, deformed, for concrete reinforcement. ASTM International, West Conshohocken.

ASTM C1437, 2015. Standard test method for flow of hydraulic cement mortar, ASTM International, West Conshohocken.

ASTM C496, 2017. Standard method of test for splitting tensile strength of cylindrical concrete specimens, ASTM International, West Conshohocken.

ASTM C348, 2021. Standard method of test for flexural strength of hydraulic-cement mortars, ASTM International, West Conshohocken.

Azhroul B.P., 2017. The effectiveness of micronized powder and crumb rubbers as fine aggregates replacement in ultra- high performance concrete. *Bachelor dissertation, University Malaysia Pahang (UMP).*

BS1881-116, 1997. Method for determination of compression strength of concrete cubes, British Standard Institute, London.

Committee, A., 2019. Building code requirements for structural concrete (ACI 318-19) and commentary, American Concrete Institute.

CAE ABAQUS. User's Manual. 2011. ABAQUS analysis user's manual.

Collins, M.P., Mitchell, D., and Macgregor, J.G., 1993. Structural design considerations for high strength concrete. *Concrete International,* 15(5), pp. 27–34.

De Brito, J., and Saikia, N., 2012. Recycled aggregate in concrete: use of industrial, construction and demolition waste, New York: Springer Science and Business Media. Doi:10.1007/978-1-4471-4540-0.

FEMA, A., 461/Interim, 2007. Testing protocols for determining the seismic performance characteristics of structural and nonstructural components, Applied Technology Council, Redwood City, CA, 113.

Iraqi specification No. 45, 1984. Aggregate from natural source for concrete, Central Agency for Standardization and Quality Control, Planning Council, Baghdad, Iraq.

Ishak, M.H.B., 2018. Chloride Resistance Penetration of Rubberized-ultra High Performance Concrete (UHPC). *Bachelor dissertation, University Malaysia Pahang (UMP).*

Kadhum, M. M., 2015. Studying of some mechanical properties of Reactive Powder Concrete using local materials. *Journal of Engineering*, 21(7), pp. 113-135. Doi:10.31026/j.eng.2015.07.09.

Kammash, K.N.A., and Abdul-Husain, Z.A., 2022. The behavior of bond strength between rebar and concrete in rubberized concrete. *Journal of Engineering*, 28(8), pp. 83-92. Doi:10.31026/j.eng.2022.08.06.

Pham, T.M., Davis, J., Ha, N.S., Pournasiri, E., Shi, F., and Hao, H., 2021. Experimental investigation on dynamic properties of ultra-high-performance rubberized concrete (UHPRuC). *Construction and Building Materials*, 307. Doi:10.1016/j.conbuildmat.2021.125104.

Richard, P., and Cheyrezy, M. H., 1994. Reactive powder concrete with high ductility and 200- 800 MPa compressive strength, Special Publication, 144, pp. 507–518.

Wang, X., Xia, J., and Li, Y., 2015. Compressive and flexural strength of Ultra-High Performance Fibre Reinforced Concrete containing recycled rubber crumb. *Sustainable Buildings and Structures,* pp. 65-70. 1st Ed., CRC Press.

Zhang, D., Li, H., Tu, H. and Weng, Y., 2022. Investigation on the quasi-static mechanical properties and dynamic compressive behaviors of ultra-high performance concrete with crumbed rubber powders. *Materials and Structures*, *55*(3), p.104. Doi:10.1617/s11527-022-01904-0